A new approach to determine nanoparticle shape and size distributions of SERS-active gold–silver mixed colloids

Nordin Félidj, Georges Lévi, Jacques Pantigny and Jean Aubard*

Institut de Topologie et de Dynamique des Systèmes (CNRS URA 34), 1, rue Guy de la Brosse, F75005 Paris, France

This paper presents new results on surface enhanced Raman spectroscopy (SERS) of various probes (pyridine, acridine) deposited onto mixed $Au_{100-x}Ag_x$ colloids constituted of gold particles overlaid by less than a single layer of silver atoms. Since both electromagnetic and chemical theories predict that the Raman enhancement depends strongly on the morphology of colloidal particles, we have used two methods to approach the particle size and shape distributions of these mixed colloids. The first one compares the profiles of the experimental and calculated extinction bands of surface plasmon resonances. The second one deals with low frequency Raman spectra from particle mechanical vibrations (*acoustic modes*). Using a recent model that we have developed to simulate the band profiles of these spectra, we can obtain the size and shape of the *resonant particles* underlying the SERS effect. These distributions, deduced from both foregoing methods, are compared with those obtained by transmission electronic microscopy (TEM) and allow us to suggest that several scales of particle sizes lead to the SERS effect. This latter result is related to the fractal nature of partially aggregated colloids displaying scale invariance. We have also analyzed the physicochemical properties of the two probes (pyridine and acridine) when they are adsorbed onto these mixed colloids. The results show that the acridine species bound to the surface depends strongly on the addition of a very small amount of silver at the gold surface. These mixed colloids allow SERS spectra of acridine to be obtained when the laser excitation takes place in the green (514.5 nm) while in pure gold colloids, acridine does not display any SERS spectrum at this excitation wavelength.

Since the discovery of surface enhanced Raman scattering (SERS) on roughened silver electrodes,[1] a great number of metallic surfaces have been investigated. Among them, we can mention island films,[2] cold deposited films,[3] colloidal suspensions[4] and more recently, colloidal films.[5,6]

Two mechanisms have been considered to account for the SERS effect. The electromagnetic mechanism (EM), arising from excitation of surface plasmon resonances localized on the roughened features, is responsible for the main enhancement and many electromagnetic theories, based on the electric dipolar approximation, have been proposed.[7–11] The second enhancement mechanism is related to the increase of the polarizability of the adsorbed molecule when a resonant charge transfer can occur between the metal and the adsorbate (chemical effect).[12] Nevertheless, this mechanism is believed to have a much smaller contribution and the overall enhancement factor generally results from both mechanisms, leading to eight orders of magnitude in favorable cases.

Since metal colloid UV/VIS spectra are related to the surface plasmon resonances, whose frequencies depend on the aggregation pattern of the sols,[4,13] the analysis of the extinction band profiles can be a way to estimate particle shape and size distributions. Thus, upon the addition of small amounts of a salt or a molecule, silver and gold colloids rapidly aggregate and display a new absorption band located at longer wavelength. As shown in Fig. 1 for gold colloids, two distributions of aggregated particles are observed, with the presence of a well-defined isobestic point at 550 nm. It has been experimentally established that strong SERS spectra are obtained only when the laser excitation takes place within the long wavelength absorption band,[13] corresponding to collective plasmon oscillations. On the other hand, if the aggregation becomes too important, the metallic particles precipitate and the SERS effect disappears. A simple method to stop colloid precipitation is to add an organic polymer [polyvinylpyrrolidone (PVP), polyvinylalcohol (PVA), *etc*]. Unfortunately, such a method leads to a decrease in the SERS intensity.

In this paper, we develop a method that allows the aggregation process[14] to be controlled by covering the gold particle surface with metallic silver atoms forming less than a single layer. The so-called $Au_{100-x}Ag_x$ colloids,[14] where the ratio x of silver can be modulated, allows the aggregation process to be monitored and yields a noticeable increase of the SERS effect for a low amount of silver.

To approach the morphology of these various Ag-clad Au colloidal composites, we have investigated mainly two tech-

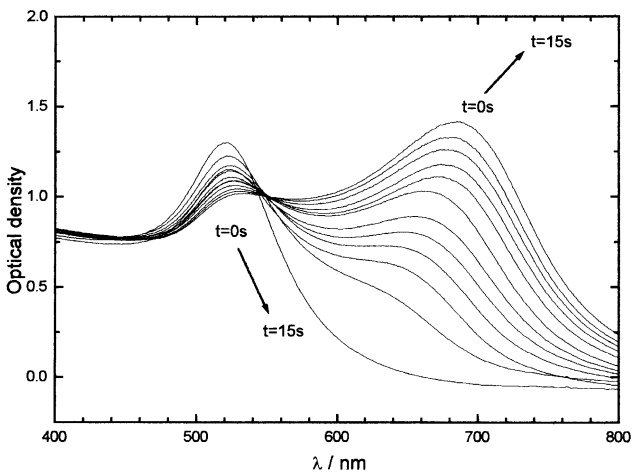

Fig. 1 Absorption spectra of Au colloids, after the addition of pyridine (2×10^{-2} M), as a function of increasing time

* Fax: +33 11 44 27 68 14; E-mail: Aubard@paris7.jussieu.fr

niques. The first one deals with the absorption spectra of these metal sols in the presence of molecular probes like pyridine and acridine. Since the maximum of the SERS intensity depends strongly on the extinction spectra profiles,[13] we have approached the morphology of the metallic clusters by comparing the experimental extinction spectra with those calculated using a simple model based on the electric dipolar approximation.[15–18] The second approach arises from the Raman spectra of the mechanical vibrations of the metallic particles themselves (*acoustic modes* or *inelastic Mie scattering*) discovered by Gersten *et al.*[19] and Weitz *et al.*[20] Indeed, these authors have shown that colloidal particles give rise to a very low frequency band due to the mechanical vibrations of metallic particles. These low frequency Raman scattering (LFRS) spectra can only be observed when they are enhanced by plasmon resonances and are thus closely related to SERS. Moreover, the acoustic bands display a shift of their maximum when the laser excitation is changed. Using a simple model, which we have previously developed[21] from dipolar electromagnetic theory,[7,8,19] we have been able to simulate the experimental LFRS profiles and thus to approach the size and shape distributions of the *resonant particles*. The comparison of these distributions with those deduced from absorption spectra and microscopic techniques, like transmission electronic microscopy (TEM), reveals significant differences, which are interpreted in terms of a scale invariance reflecting the fractal nature of the partially aggregated colloids.

In the last part of this article, to get more insight on the particular properties of the Ag–Au mixed colloids, SERS, LFRS and UV/VIS extinction spectra have been recorded in the presence of acridine. Comparison with the data for the pure Au and Ag colloids obtained under the same experimental conditions reveals that the SERS intensity variations in the composites are not only due to Ag inhibition of the Au particle aggregation. The SERS experiments with acridine also indicate that the observed spectral changes probably arise from a deep perturbation of the electrochemical characteristics of these surfaces.

Experimental

Absorption measurements in the region from 350 to 950 nm have been carried out on a Perkin Elmer (Lambda 2) UV/VIS spectrophotometer.

SERS spectra of pyridine and acridine were recorded in the backscattering geometry on a DILOR XY spectrometer using an excitation line at either 632.8 nm of a HeNe model 207B Spectra Physics laser (25 mW power at the laser head) or at 514.53 nm of an Ar^+ model 165 Spectra Physics laser (power less than 50 mW). Briefly, the spectrometer is constituted of a double monochromator used in subtractive mode to select a given spectral range, followed by the spectrograph to complete the dispersion, and a Jobin–Yvon CCD matrix cooled thermoelectrically. The low frequency Raman spectra were recorded in backscattering geometry on the same apparatus but with the double monochromator set in additive mode and a cooled 9558 EMI photomultiplier associated with photocounting techniques used as a single channel detector. Using 60 or 80 μm slit widths, the spectral resolution was always less than about 1 cm^{-1} and the rejection of the elastic scattering was good enough to allow the recording of Raman spectra down to 2 cm^{-1} from the Rayleigh line.

Transmission electronic microscopy (EM 912 Omega, Zeiss Twins) plates were taken in air by evaporating a small colloid drop on a carbon grid covered with collodion.

Ag-clad Au colloids were prepared according to the Freeman *et al.* procedure,[14] which is not reported here. The TEM plates showed no difference between pure Au and $Au_{100-x}Ag_x$ sols for $1 \leqslant x \leqslant 10$. All colloidal particles are almost of spherical shape with a narrow diameter distribution ranging from 10 to 15 nm.

Results and Discussion

Brief description of the model used to simulate experimental extinction profiles

Since the early work of Maxwell–Garnett[22] and Mie,[23] metal colloidal particles have attracted much attention both experimentally and theoretically. The theoretical appeal arises from the many fascinating electrical and optical properties of metal particles that are different from bulk metal. For instance, the color of gold, silver and copper colloids has been explained to be due to surface plasmon resonances of the conducting electrons. Metallic particles are also of practical interest because of their small size and large surface area compared to bulk metal. This large surface is highly desirable in diverse applications such as heterogeneous catalysis or SERS. Indeed, upon addition of organic molecules and ions (or electrolytic salts), the colloid aggregates, thus giving rise to new absorption bands underlying the SERS effect.

In this section we describe a simple model, based upon the dipolar electromagnetic theory given by Maxwell[15] and Lord Rayleigh,[16] to account for the light scattering by spheroids, the size of which is small compared with the wavelength. This model, which has been developed in order to calculate extinction profiles that can be fitted to the experimental ones, is based upon the following assumptions.

(*i*) Due to the low concentration in gold, the particles are far enough from each other to admit that they scatter light in an independent way. The resulting extinction cross section, C_T, can therefore be considered as a suitably weighted sum of various extinction cross sections $C_{ext}(i)$:

$$C_T = \sum_i w_i C_{ext}(i) \tag{1}$$

(*ii*) The aggregation of the colloid is low enough to consider that all aggregates remain very small compared to the incident wavelength. A check of this approximation is given by TEM micrographs, which show that, when deposited onto a copper grid covered with collodion, the aggregates remain smaller than the wavelength [Fig. 2(*a*)]. However, these TEM pictures do not reflect the genuine aggregation pattern of the colloidal sols. Indeed, it is quite likely that deposition and evaporation of the colloid onto the grid lead to additional aggregation. It is thus reasonable to consider that the clusters in the colloidal sols are much smaller than those observed by TEM and thus very small with respect to the wavelength, thus justifying the dipolar approximation. Furthermore, as shown in Fig. 2(*a*) the clusters of the deposited colloid appear as objects of elongated shape. According to the above mentioned reasons, the aggregates within the colloidal sols are likely to be formed by a small number of spherical particles, and thus can be mimicked as spheroids of various ratios, $r = a/b$, of the semi-major axis a to the semi-minor axis b.

(*iii*) The absorption C_{abs} and scattering C_{scat} cross sections of the various ellipsoids are calculated using the electric dipolar approximation,[15–18] that is when the particle sizes are much smaller than the analyzing radiation wavelength:

$$C_{abs} = \frac{8\pi^2}{3\lambda} \mathrm{Im}(\alpha_\ell + 2\alpha_t), \tag{2}$$

$$C_{scat} = \frac{128\pi^5}{9\lambda^4} (|\alpha_\ell|^2 + 2|\alpha_t|^2), \tag{3}$$

$$C_{ext} = C_{abs} + C_{scat} \tag{4}$$

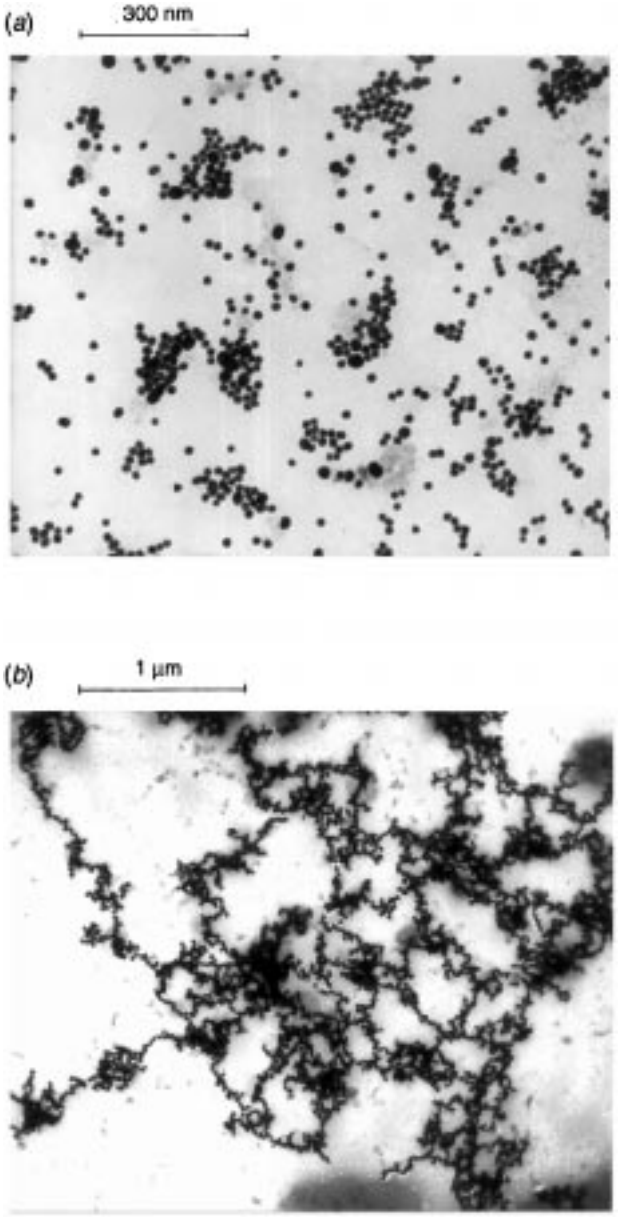

Fig. 2 (*a*) TEM image of $Au_{95}Ag_5$ colloids, in the presence of pyridine (2×10^{-2} M); (*b*) TEM image of pure Au colloids, under the same conditions

In the above equations [eqn. (2)–(4)], α_ℓ and α_t denote respectively the longitudinal and the transversal polarizability tensor components given by

$$\alpha_{\ell,t} = \frac{V(\varepsilon - 1)}{4\pi + (\varepsilon - 1)P_{\ell,t}}, \quad (5)$$

where $V = (4/3)\pi ab^2 = (4/3)\pi rb^3$ is the volume of the spheroid, ε is the dielectric constant of the metal with respect to the surrounding medium and $P_{\ell,t}$ is a shape factor given by[15–18]

$$P_\ell = \frac{4\pi}{r^2 - 1}\left\{\frac{r}{\sqrt{r^2 - 1}}\ln[r + \sqrt{r^2 - 1}] - 1\right\}, \quad (6)$$

$$P_t = \frac{4\pi - P_\ell}{2} \quad (7)$$

The fitting of the normalized extinction profiles is performed by determining the weight w_i of each extinction coefficient $C_{ext}(i)$ that gives the best possible agreement between the calculated and experimental curves. This procedure is achieved using the Simplex minimization method,[24] which consists in a series of geometric operations using a multi-parameter function. This best weight, when normalized to 100, gives the percentage of spheroids of ratio $r = a/b$. In our computation, we have fixed the semi-minor axis b to the mean radius of individual particles, 5 nm, and we have varied r from 1.0001 (sphere) to 10. The values of the dielectric constant used in these computations were those of gold with respect to water and were taken from the Johnson and Christy tables.[25] The justification for this choice is given hereunder.

Comparison between experimental and calculated extinction profiles. Size distributions of Ag-clad Au colloids

The extinction spectra of unaggregated mixed colloids of $Au_{100-x}Ag_x$ (*i.e.*, in the absence of any probe) are indiscernible from those observed for pure gold colloids as long as x, the silver amount, remains lower than ten percent.[14] In these cases, only the gold plasmon resonance at 520 nm is visible, contrary to the corresponding mixtures of Au and Ag colloids where the sharp silver plasmon resonance at 390 nm is clearly apparent.[14] These observations support the choice of the gold dielectric constant with respect to water in all our calculations.

Experimental extinction spectra of $Au_{100-x}Ag_x$ colloids obtained after the addition of pyridine (2×10^{-2} M) and recorded at the completion of the aggregation process (a few minutes) are displayed in Fig. 3 for the silver percentage x ranging between 0 and 5. For pure gold colloids ($x = 0$), the long wavelength band is shifted to very large λ values and is very broad with a maximum located at approximately 780 nm. As x increases, this long wavelength band becomes sharper and less shifted with respect to the short wavelength one. When $x = 5$, only a shoulder is observed on the long wavelength wing of the plasmon resonance at 520 nm; lastly, when $x \geqslant 6$, the extinction spectra is quite similar to that of the unaggregated gold colloid.[13,14] These results are qualitatively interpreted as a progressive inhibition of the aggregation process upon the addition of silver atoms at the gold surface. We will see, in the following section, that the intensity of the SERS spectrum of pyridine reaches its maximum when the laser excitation is close to the maximum of the long wavelength band.

The simulation of the extinction band profiles of these aggregated colloids, by the method described in the previous section, quantitatively confirms this conclusion. As shown in Fig. 4(*a*) and 4(*c*), this method gives a rather good fit between experimental and calculated profiles. The distributions of the r ratios for $Au_{95}Ag_5$ [Fig. 4(*b*)] and $Au_{98}Ag_2$ [Fig. 4(*d*)] are constituted of two parts: a very narrow distribution centered at $r \simeq 1.3$–1.5, which is associated with unaggregated particles, and a much broader distribution ranging over large r values due to various aggregates. When the aggregation is rather low, as shown in Fig. 4(*a*) for $Au_{95}Ag_5$, the total amount of clusters ranging up to $r \approx 3.5$ remains below 25%. On the other hand, when the aggregation is more important, as clearly evidenced in Fig. 4(*c*) for $Au_{98}Ag_2$ by the presence of the broad long wavelength band centered at 740 nm, the amount of clusters with large r values is approximately 50% and the distribution extends to $r \approx 6$.

The TEM micrographs of pure gold colloids aggregated with pyridine reveal large fractal aggregates with a Hausdorff dimension[26] of $d = 1.75$ [Fig. 2(*a*)]; these aggregates are much larger than those observed on the micrographs obtained from $Au_{95}Ag_5$ colloids under the same experimental conditions [Fig. 2(*b*)]. These observations are in agreement with the conclusions drawn from extinction spectra analysis.

SERS spectra of pyridine on Ag-clad Au colloids

As pyridine is the most famous probe used to test SERS, we have recorded its Raman spectrum when deposited onto various $Au_{100-x}Ag_x$ mixed colloids using 514.53 and 632.8

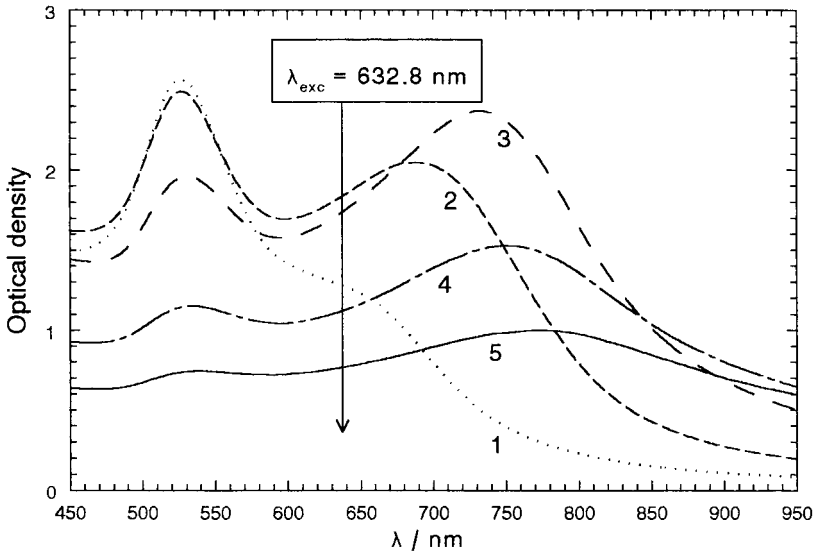

Fig. 3 Extinction spectra of various $Au_{100-x}Ag_x$ mixed colloids, after addition of pyridine (2×10^{-2} M): 1 (·····) $Au_{95}Ag_5$, 2 (– – – –) $Au_{97}Ag_3$, 3 (— —) $Au_{98}Ag_2$, 4 (—·—) $Au_{99}Ag_1$, 5 (———) Au_{100}

nm laser excitation. However, SERS spectra were obtained only when the laser excitation took place at 632.8 nm; no signal could be detected using the 514.53 nm excitation line even when long integration times were used. When exciting at 632.8 nm, as shown in Fig. 5, the SERS integrated intensity of the 1008 cm^{-1} pyridine line was found to depend on the concentration x of silver.[14] We notice that this intensity is almost the same for $x = 1$, 2 and 3, corresponding to similar long wavelength resonances (Fig. 3). For pure gold colloid ($x = 0$), the weakening of the SERS intensity is due to the broad and long wavelength shifted absorption band. On the other hand, the very poor intensity of the SERS spectrum for $x = 5$ results from the weaker aggregation of the colloid as shown for example in Fig. 4(*a*), (*b*). Indeed, comparison between TEM micrographs of deposits of $Au_{95}Ag_5$ and Au_{100} colloids confirms the lower degree of aggregation of the composite than that of pure gold colloid (Fig. 2).

Acoustic modes on gold colloids

Gersten *et al.*[19] and Weitz *et al.*[20] have observed that mechanical vibrations of silver surface protrusions or colloidal particles can give rise to a low frequency Raman scattering (LFRS) band located at approximately 10 cm^{-1}, provided the intensity of this band is suitably enhanced by surface plasmon resonance excitation. These LFRS bands, also called *acoustic modes*, display some interesting properties: the band maximum depends on the laser excitation wavelength and on the refractive index of the medium surrounding the metallic particles. Furthermore, the intensity of these acoustic modes is increased when a molecule, like pyridine for example, is adsorbed onto the surface. In order to account for these bands and their properties, these authors[19,20] developed a model, based on the Gersten and Nitzan[7] theory of SERS in which surface protrusions or colloidal particles are mimicked as (hemi)spheroids, and thus determined the Raman differential cross section, $d\sigma/d\bar{\omega}$, of the (hemi)spheroid covered by a single molecule. The maximum Ω_{max} of the band, given by

$$\Omega_{max}(cm^{-1}) \simeq \frac{v}{2ac} \quad (8)$$

where v is the sound velocity in the metal, c the speed of light and a the semi-major axis of the spheroid, was found to depend on the excitation wavelength due to the simultaneous mechanical [eqn. (8)] and electromagnetic (plasmon) resonances. Recently, we have proposed a model that allows the calculation of acoustic band profiles in good agreement with experimental ones, and the determination of the resonant metallic particle size distributions.[21] Moreover, we have enlightened the relation between LFRS, SERS and absorption spectra.[27]

In the presence of pyridine, the LFRS from acoustic modes of Ag-coated Au particles were hardly detectable at 632.8 nm and we present here the results obtained in pure Au colloids. On the other hand, good quality LFRS spectra were obtained with acridine; they will be presented and analyzed further on in this paper. In the following we show that the simulation of acoustic band profiles can be used to determine the resonant particle size distribution of gold. For this purpose the scattered intensity, $\mathcal{I}_\Omega$, is assumed to be proportional to

$$\mathcal{I}_\Omega \propto \mathcal{N} \frac{d\sigma}{d\bar{\omega}} \quad (9)$$

where $\mathcal{N}$ is the number of resonant spheroids of a given semi-major axis a and $d\sigma/d\bar{\omega}$ is the Raman differential cross section calculated by Gersten *et al.*[19] and Weitz *et al.*[20] If the probability that $\mathcal{N}$ particles have a given value of the semi-major axis a is assumed to be a Gaussian distribution, $\mathcal{G}(a_0, \Delta a)$, centered at a_0 and of standard deviation Δa, the simulation of the experimental LFRS band profile, obtained by fitting a_0 and Δa, leads to the resonant particle size distribution, $\mathcal{G}(a_0, \Delta a)$.

Fig. 6 compares the acoustic mode profile obtained from a gold colloid in the presence of pyridine (10^{-2} M), and its simulation using our model.[21] To our knowledge, it is the first time that such an acoustic mode is observed for a gold colloid. The agreement between experimental and calculated profiles appears satisfactory except for the contribution of the huge Rayleigh line. The $a_0 = 2.5$ nm and $\Delta a = 6.6$ nm parameters give the relevant features of the resonant particle size distribution.

It should be pointed out that the semi-major a and semi-minor b axes values of the spheroid, obtained by this technique, are smaller than the mean radius of individual gold particles, which is approximately 5 nm. Therefore, we attribute the LFRS band to localized plasmon resonances of *nanostructures* due to the very disorganized nature of the aggregated colloid.[27] The comparison of these results with those obtained from other techniques (SERS, UV/VIS extinction bands, TEM) suggests there are several scales of particles underlying the Raman enhancement process. These different scales may reflect the fractal nature of aggregated colloids.[26]

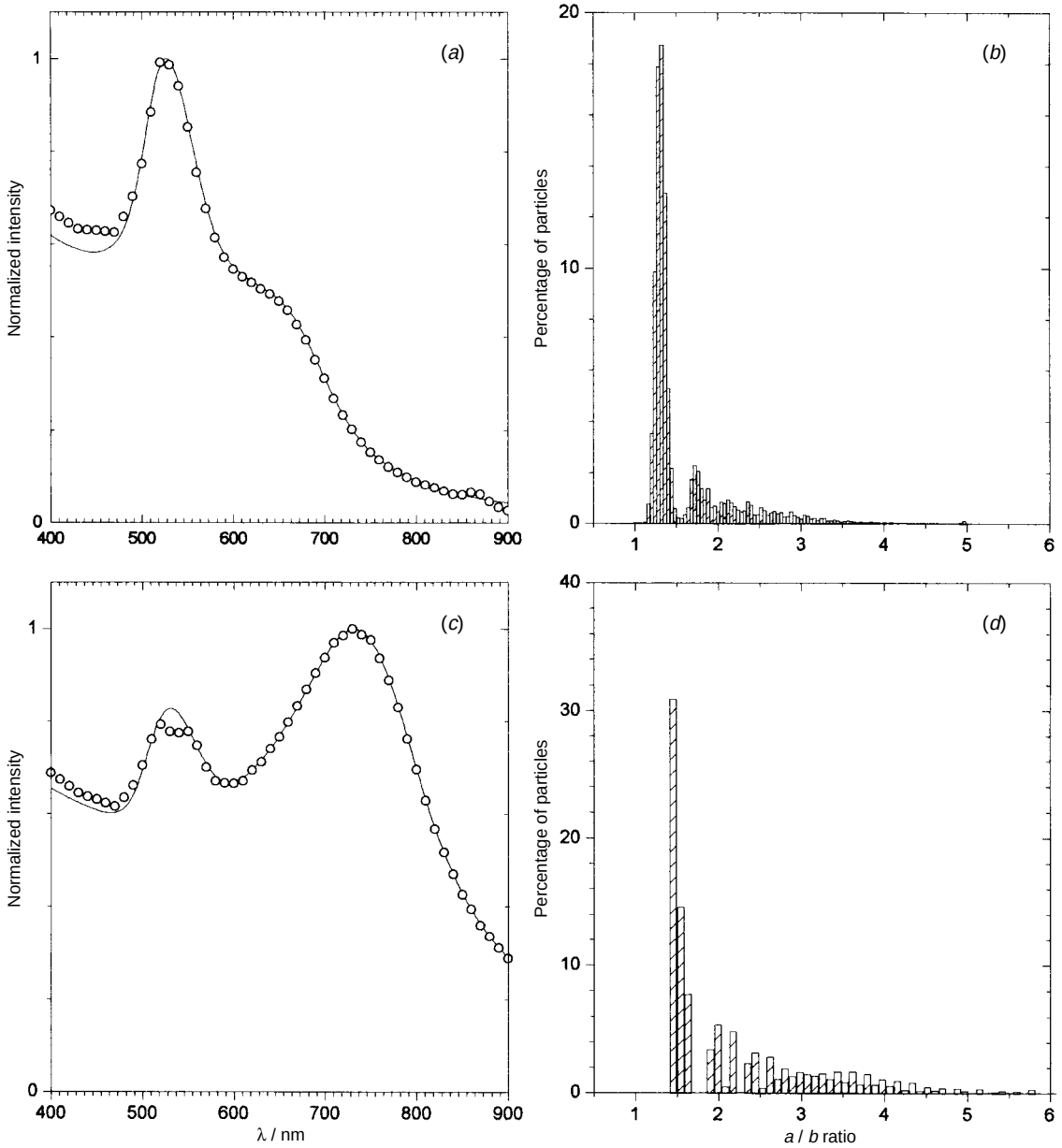

Fig. 4 Simulation of experimental extinction profiles and cluster shape distributions for $Au_{95}Ag_5$ [(*a*) and (*b*)] and $Au_{98}Ag_2$ [(*c*) and (*d*)], in the presence of pyridine (2×10^{-2} M)

Au–Ag mixed colloids in the presence of acridine: SERS, LFRS and extinction spectra

In the foregoing section, we have been able to determine the various scales of the size distribution of the aggregated gold particles in the presence of small amounts of silver. The results of band simulations of either LFRS or absorption profiles clearly indicate that addition of silver atoms at the gold surface, even at less than a monolayer ($x \leqslant 5$), leads to inhibition of the pyridine-induced aggregation. Since colloid aggregation is the main condition for SERS enhancement (through the EM mechanism), we have actually demonstrated that the strongest intensities of pyridine SERS lines were related to the presence of the long wavelength plasmon band. The disappearance of this band for $x > 5$ (Fig. 3) corresponds to an important decrease in the aggregation of gold colloids leading to the concomitant quenching of the pyridine SERS spectrum (Fig. 5).

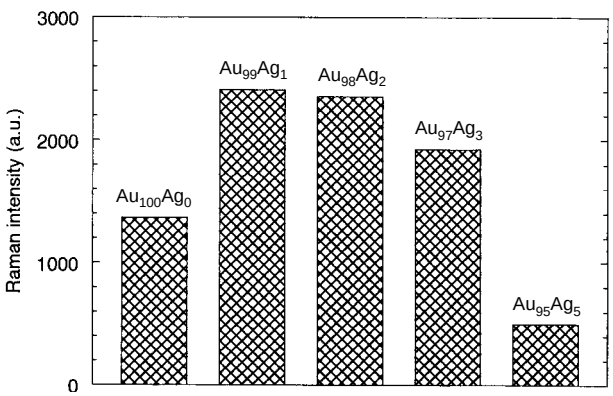

Fig. 5 SERS integrated intensity of the 1008 cm^{-1} pyridine line for various $Au_{100-x}Ag_x$ mixed colloids (concentration: 2×10^{-2} M; 632.8 nm laser excitation)

Although these pyridine SERS experiments clearly indicate that the variations in SERS intensity in the mixed Au–Ag colloids are due to changes at the particle surface, they give no information concerning the metal adsorbate interaction. To determine whether the adsorbate is interacting with Au or surface-bound Ag particles, we used acridine, a molecule whose protonation equilibrium at the surface is very sensitive to the electrolytic surrounding of the metal.[28,29] Fig. 7 compares the SERS spectra, excited at 632.8 nm, of acridine

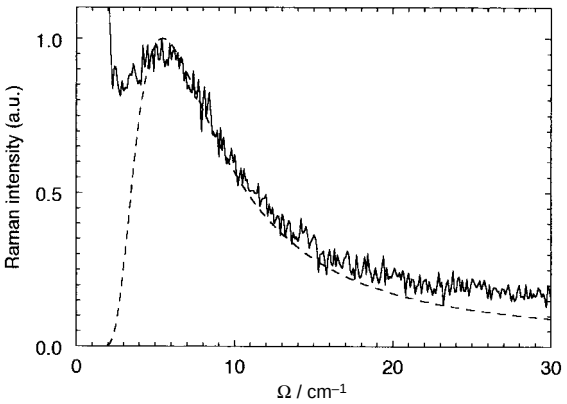

Fig. 6 Experimental and calculated low frequency Raman mode from gold colloids in the presence of pyridine (10^{-2} M; 632.8 nm laser excitation). ——— experimental curve, – – – – calculated curve

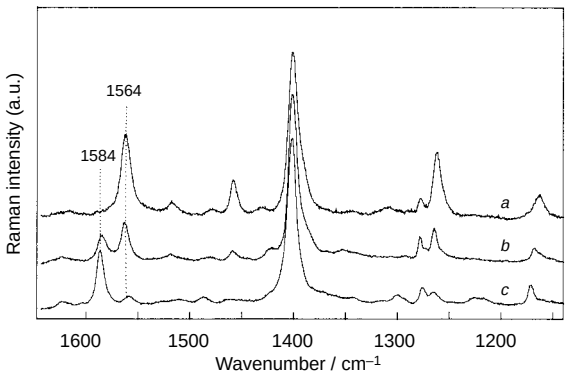

Fig. 7 SERS spectra of acridine (5×10^{-6} M, 632.8 nm laser excitation) in (curve *a*) gold colloid, (curve *b*) silver colloid, (curve *c*) $Au_{98}Ag_2$ mixed colloid

(5×10^{-6} M) adsorbed on gold colloid (curve *a*), silver colloid (curve *b*), and $Au_{98}Ag_2$ mixed colloid (curve *c*). All these spectra were obtained at pH approximately equal to 7–7.5 and in the presence of chloride ions (typically 4–10 mM) coming either from the colloidal preparation (for Au and mixed colloids) or added after the preparation (for silver colloids). From the analysis of the lines at 1584 and 1564 cm^{-1}, characteristic of the protonated (AH^+) and neutral species (A), respectively, we observe that the AH^+ species contributes to

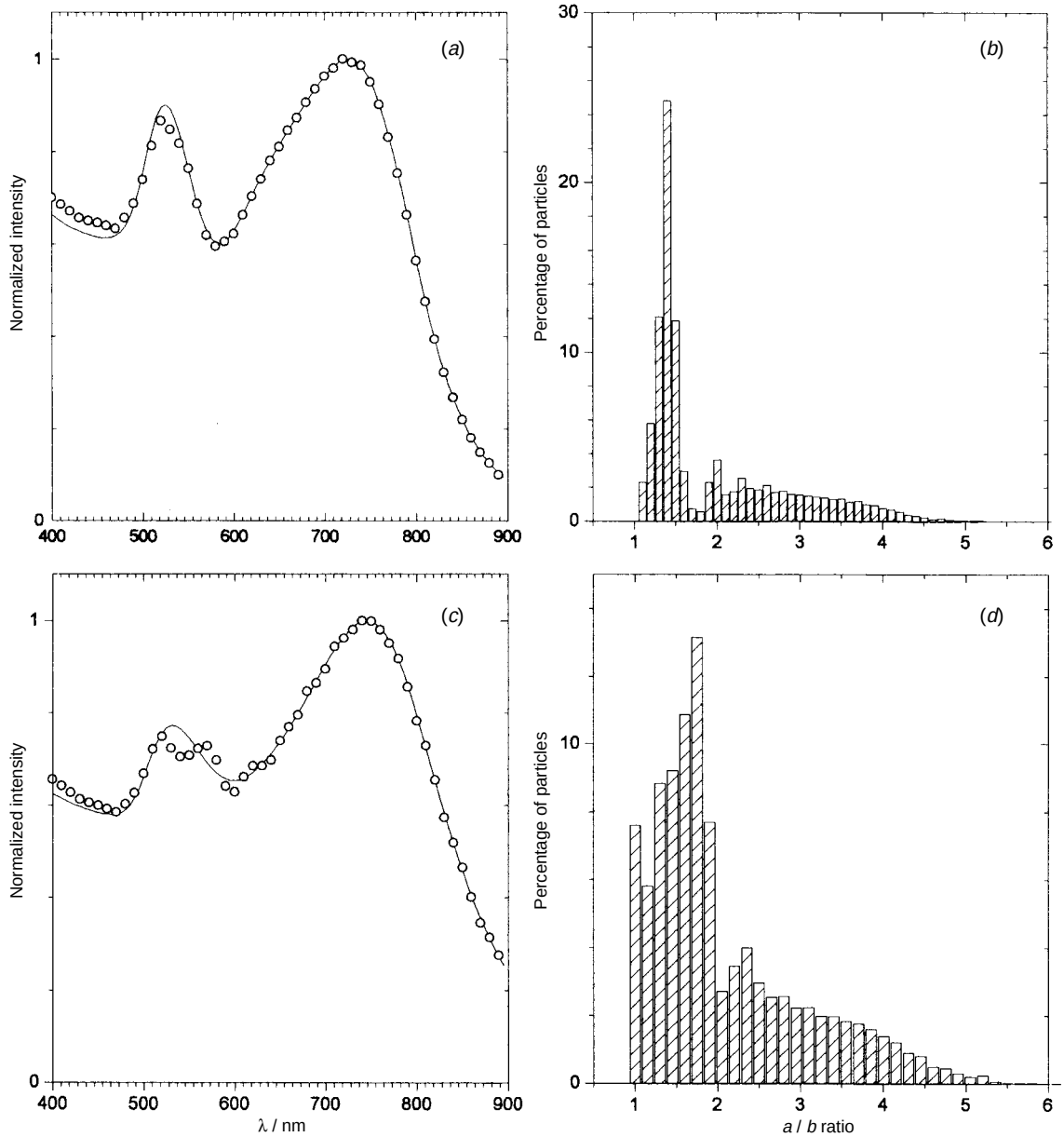

Fig. 8 Simulation of experimental extinction profiles and cluster shape distributions for $Au_{98}Ag_2$ [(*a*) and (*b*)], and Au_{100} [(*c*) and (*d*)], in the presence of acridine (5×10^{-6} M)

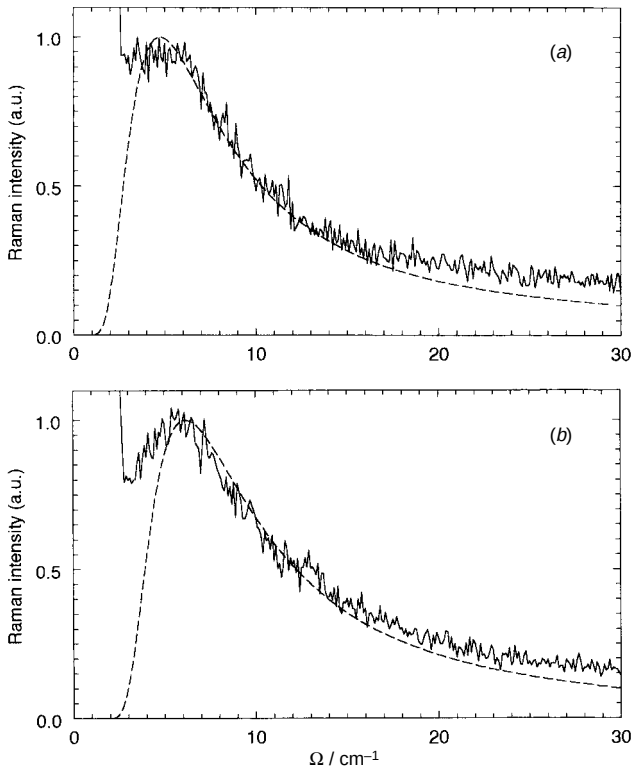

Fig. 9 Experimental and calculated low frequency Raman bands from (*a*) Au_{100} and (*b*) $Au_{98}Ag_2$ colloids, in the presence of acridine (5×10^{-6} M, 632.8 nm laser excitation). ——— experimental curve, – – – – calculated curve

the SERS spectra for the Ag and Ag-clad Au surfaces, while only the neutral species give rise to a SERS spectrum on Au colloids. These data strongly suggest that, under the present experimental conditions, acridine is mainly adsorbed as the acridinium cation onto the small Ag particles in the mixed Au–Ag colloids.

Moreover, while for pyridine no SERS effect was detected at 514.5 nm, even for the most SERS-active Au–Ag composites (*i.e.*, $Au_{97}Ag_3$ to $Au_{99}Ag_1$), in the case of acridine good quality SERS spectra, excited at this wavelength, were obtained with these substrates (not shown). As previously suggested, this enhancement towards the blue for the SERS acridine spectrum originates from a resonant charge transfer due to the formation of an ion pair, AH^+–Cl^-.[28,29] This hypothesis reinforces the argument in favor of a direct adsorption of acridinium species on Ag in mixed colloids.

All these observations are in agreement with the previous SERS results of Freeman *et al.*,[5] for the adsorption of *para*-nitroso-*N*,*N*′-dimethylaniline (another protonatable species) in Ag–Au colloids.

The extinction profiles for Au_{100} and $Au_{98}Ag_2$ colloids in the presence of acridine are shown in Fig. 8(*a*) and 8(*c*), along with the simulated profiles. It should be noticed that, although the experimental spectra are rather similar to the corresponding ones seen for pyridine (Fig. 4), the obtained $r = a/b$ distributions are different, thus reflecting the sensitivity of our simulation method. Once again, very small amounts of Ag ($x \leqslant 5$) lead to a progressive inhibition of adsorbate-induced aggregation with a slight blue shift of the long wavelength plasmon band (from 750 to 730 nm). This is clearly evidenced by the distribution of the ratios r deduced from the simulation [Fig. 8(*b*) and 8(*d*)]. This feature allows a better matching of the 632.8 nm laser excitation to the long wavelength plasmon resonance band, thus allowing the SERS intensity to be monitored.

The LFRS for Au_{100} and $Au_{98}Ag_2$ colloids in the presence of acridine, excited at 632.8 nm, are presented in Fig. 9. From the simulation of the profiles, the Gaussian center and the standard deviation have been estimated to be $a_0 = 2$ nm and $\Delta a = 5.1$ nm for Au_{100} colloid, and $a_0 = 2$ nm and $\Delta a = 5.7$ nm for $Au_{98}Ag_2$ colloid. Here again, they are smaller than the dimensions of individual gold particles, reinforcing the suggestion that nano-protrusions are at the origin of SERS.

Since there is a close relationship between the SERS effect and the acoustic mode, we attempted to detect LFRS from $Au_{98}Ag_2$ acoustic vibrations in the presence of acridine, but excited at 514.5 nm within the plasmon resonance band of silver particles. Indeed, the observation of a SERS effect at this wavelength has led us to consider that LFRS could be detected under these conditions, thus providing direct *in situ* information on the shape and size distributions of the resonant Ag-clad Au particles. Unfortunately, even using long photo-counting integration times, no acoustic mode was detected. This indicates that the morphological information (shape and size) deduced from the modelisation of either extinction or LFRS profiles are only relevant to the aggregation pattern of gold particles.

Conclusion

The present study of SERS spectra of pyridine and acridine, along with the extinction spectra of various $Au_{100-x}Ag_x$ mixed colloids, brings some new information on the morphology of the colloidal gold clusters leading to the SERS effect.

The simulation of the extinction spectra in the presence of pyridine and acridine allowed us to give an approach of the $r = a/b$ ratio distributions for the spheroids modelising the particle clusters. Comparison of these distributions with those deduced from the simulation of the low frequency Raman bands (mechanical vibrations of the particles) reveals the presence of nano-protrusions and suggests that several size distributions are underlying the SERS effect. We conclude that, for such disorganized substrates like partially aggregated colloids, the SERS effect originates from the coupling, over the whole cluster, between the molecules and these nanostructures. The fractal nature of aggregated colloids could also play a significant role.[30–32]

The analysis of the SERS spectra of acridine indicates that this molecule is specifically adsorbed as the acridinium species onto the silver particles of Au–Ag composites. This result, along with those deduced from band simulations (absorption and LFRS), suggests that Ag-clad Au, even at low Ag coverage, perturbs the Au colloidal aggregation and leads to a modification of the electrochemical double layer.

We are now investigating silver and gold colloidal films giving rise to strong enhancement of Raman scattering.[5,6] These quite stable new substrates will be developed in order to analyze the coloring mechanisms and the degradation processes of photochrome compounds.

References

1 M. Fleischmann, P. J. Hendra and A. J. McQuillan, *Chem. Phys. Lett.*, 1974, **26**, 163.
2 C. A. Murray and D. L. Allara, *J. Chem. Phys.*, 1982, **76**, 1290.
3 M. Moskovits and D. P. Di Lella, *J. Chem. Phys.*, 1982, **73**, 4408.
4 J. A. Creighton, C. G. Blatchford and M. G. Albecht, *J. Chem. Soc., Faraday Trans. 2*, 1980, **75**, 790.
5 R. G. Freeman, K. C. Grabar, K. J. Allison, R. M. Bright, J. A. Davis, A. P. Guthrie, M. B. Hommer, M. A. Jackson, P. C. Smith, D. G. Walter and M. J. Natan, *Science*, 1995, **267**, 1629.
6 G. Chumanov, K. Sokolo, B. W. Gregory and M. T. Cotton, *J. Phys. Chem.*, 1995, **99**, 9466.
7 J. I. Gersten and A. Nitzan, *J. Chem. Phys.*, 1980, **73**, 3023.
8 J. I. Gersten and A. Nitzan, *J. Chem. Phys.*, 1981, **75**, 1139.
9 M. Moskovits, *J. Chem. Phys.*, 1978, **69**, 4159.
10 S. L. McCall, P. M. Platzman and P. A. Wolff, *Phys. Lett.*, 1980, **77**, 381.
11 P. K. Aravind and H. Metiu, *Chem. Phys. Lett.*, 1980, **74**, 301.
12 A. Otto, *J. Raman Spectrosc.*, 1991, **22**, 743.

13 J. A. Creighton, in *Surface Enhanced Raman Spectroscopy*, ed. R. K. Chang and T. E. Furtak, Plenum, New York, 1982, pp. 315–337.
14 R. G. Freeman, M. B. Hommer, K. C. Grabar, M. A. Jackson and M. J. Natan, *J. Phys. Chem.*, 1996, **100**, 718.
15 J. C. Maxwell, in *A Treatise on Electricity and Magnetism*, 3rd edn., Oxford University Press, Oxford, 1892, vol. II, pp. 66–70.
16 Lord Rayleigh, *Philos. Mag.*, 1897, **44**, 28.
17 M. Kerker, *The Scattering of Light and other Electromagnetic Radiation*, Academic Press, London, 1969.
18 H. C. van de Hulst, *Light Scattering by Small Particles*, Dover Publications, New York, 1981.
19 J. I. Gersten, D. A. Weitz, T. J. Gramila and A. Z. Genack, *Phys. Rev. B*, 1980, **22**, 4562.
20 D. A. Weitz, T. J. Gramila, A. Z. Genack and J. I. Gersten, *Phys. Rev. Lett.*, 1980, **45**, 355.
21 N. Félidj, J. Aubard and G. Lévi, *J. Chem. Phys.*, 1996, **104**, 9735.
22 J. C. Maxwell-Garnett, *Philos. Trans. R. Soc. London, A*, 1904, **203**, 385.
23 G. Mie, *Ann. Phys. Leipzig*, 1908, **25**, 377.
24 J. A. Nelder and R. Mead, *Comput. J.*, 1965, **7**, 308.
25 P. B. Johnson and R. W. Christy, *Phys. Rev. B*, 1972, **6**, 4370.
26 D. A. Weitz and M. Oliviera, *Phys. Rev. Lett.*, 1984, **52**, 1433.
27 N. Félidj, Thèse, Université Pierre et Marie Curie Paris VI, 1997 (available on request to the author).
28 S. T. Oh, K. Kim and M. S. Kim, *J. Phys. Chem.*, 1991, **95**, 8844.
29 G. Lévi, J. Pantigny, J. P. Marsault and J. Aubard, *J. Raman Spectrosc.*, 1993, **24**, 745.
30 V. A. Markel, L. S. Muratov, M. I. Stockman and T. F. George, *Phys. Rev.*, 1991, **43**, 8183.
31 M. I. Stockman, V. M. Shalaev, M. Moskovits, R. Botet and T. F. George, *Phys. Rev.*, 1992, **46**, 2821.
32 D. P. Tsaï, J. Kovacs, Z. Wang, M. Moskovits, V. M. Shalaev and R. Botet, *Phys. Rev. Lett.*, 1994, **72**, 4149.

Received in Montpellier, France, 24th October 1997;
Paper 7/09242C